

V.V. Bryukhovetsky¹, V.V. Lytvynenko¹, D.E. Myla¹, V.A. Bychko², Yu.F. Lonin³,
A.G. Ponomarev³, V.T. Uvarov³

Effect of Structural and Phase Changes under Relativistic Electron Pulsed Beam Irradiation on the Aluminum Alloys Micro-hardness

¹*Institute of Electrophysics and Radiation Technologies NAS of Ukraine, Kharkiv, Ukraine, ntcefo@yahoo.com*

²*Chernihiv National University of Technology, Chernihiv, Ukraine*

³*NSC «Kharkiv Institute of Physics and Technology» NAS of Ukraine, Kharkiv, Ukraine*

The paper studies the distinctive features of micro-hardness value changes in the zone of industrial aluminum alloy 1933 and alloy 1380 irradiated by the relativistic electron beam. The surface layer was modified under the relativistic electron beam injected along with the equal energy parameters. However, we have to claim that some physical and technological properties of the irradiated alloys layer came with some differences. The modified layer micro-hardness increased over 30 % in 1933 aluminum alloy and decreased by 10 % in 1380 aluminum alloy. The mechanisms affecting the metal material strengthening transformation after a pulsed electron beam application are analyzed. Thus, it was established that one of the core impacts to increase the micro-hardness of 1933 aluminum alloy surface layer was fine MgO impurities being absent in the initial alloy and caused by the irradiation, whilst the micro-hardness of the irradiated layer of the 1380 aluminum alloy decreases due to the dissolution during irradiation of the strengthening phases, which were identified in the initial state.

Keywords: micro-hardness, irradiation, structural-phase changes, aluminum alloys.

Received 12 May2021; Accepted 1 October2021.

Introduction

The rapid growth of the nuclear, aerospace, and automotive industries creates a great demand for engineering materials with high-performance properties. The target aluminum alloys (1933 and 1380 [1, 2]) referring to this group of materials are the subject to be studied in this paper. We can apply these alloys to produce large forging and stamping as well as heavily loaded machine parts. These alloys obtain a high strength-to-weight ratio, although they require advanced processing techniques to produce semi-finished products. The application of various heat treatment types makes you able to manage a wide range of aluminum alloy performance properties required by their area of use. Recently was established that of the 1933 aluminum alloy manifested the superplasticity effect [3, 4].

But we have to admit that the alloys do not come

along with only pros but as well as contras. These alloys show poor wear and corrosion resistance. Today we have a vast many of surface treatment and alloy strengthening methods to improve their performance properties. One of such methods is a method of the surface treatment with the intense pulsed electron beams (IPEB), but this method is in the process to be developed [5-13]. The surface treatment with IPEB essence is an energy transfer from the source (of energy, radiation, heat, or mechanical shock) onto the irradiated surface to gain improved properties due to the intense localized affecting. Whilst IPEB affecting the temperature of the alloy surface layer is increasing rapidly (achieving the melting point) with the further rapid cooling transferring the heat to host metal which remains almost cold. The alloy surface layer subjected to irradiation comes through the melting process, redistribution of the alloying element, ablation, ultrafast melt crystallization, transformations of phase composition and dislocation structure, dislocation density

increasing, grain size alteration, and emerging of residual stress [5-11]. Up to present mechanisms, responsible for the emerging of a target surface layer microstructure after IPEB irradiation, requires further investigation. The understudied issue of the matter is the as-cast chemical and phase compound influence on the micro-hardness in the IPEB remelted surface layer. Moreover, the change of strength characteristics of the surface layer after IPEB irradiation is ambiguous. The micro-hardness values in the modified surface layer can remain unchanged, increase or decrease [6,7]. Such micro-hardness behavior can be explained in collecting of the point and line defects at the phase compound transformation after IPEB irradiation. This paper will focus on studying and analyses of the micro-hardness values of the modified surface layers after IPEB irradiation of alloy 1933 and alloy 1380. The target alloys choice is stipulated by the availability of the same alloying elements that may influence the structure state and phase compound.

I. Experimental Procedure

The specimens produced of the serial semi-finished products subjected to irradiation in TEMP-A accelerator with energy flux density 10^9 W/cm^2 (electron energy $-E_n \approx 0,3 \text{ MeV}$, the current $-I_n \approx 2 \text{ kA}$, pulse duration $\tau_i \approx 5 \cdot 10^{-6} \text{ c}$, beam diameter $D \approx 3 \text{ cm}$) [5, 9,11]. The specimen irradiation was performed at the base of the NSC KIPT (the National Science Center 'Kharkiv Institute of Physics and Technology' NAS of Ukraine).

The grain microstructure research was carried out with the optical microscope MIM-10 and the scanning electron microscope TESCAN VEGA3 LMH and the optical. Keller's reagent revealed the grain microstructure on the polished etched surface. X-Ray structure analysis was carried out by DRON 4-07 diffractometers. To identify the grain microstructure parameters we applied XRD pattern full-profile analysis

with the application of regular software. The chemical composition of local micro-volumes of alloys was determined using a Tescan VEGA 3 LMH raster electron microscope with a prefix for X-ray energy dispersion microanalysis of the Bruker XFlash 5010 system. The micro-hardness tester PMT-3M was applied to confirm the micro-hardness changes under the Vickers micro-hardness (HV) with a force application of 50 g.

II. Results

The paper focused mainly on examining aluminum alloy 1380 (comparable to alloy AK8) and alloy 1933. For the purpose of the paper and to conduct the experiments, we fabricated the specimens of 1.5 mm in length. Table 1 shows chemical composition of 1933 and 1380 aluminum alloys. Although the alloys come with the same alloying elements, the core elements for every alloy considerably varies e.g. Zn and Mg are the ones for alloy 1933 and Cu and Si - for alloy 1380.

The surface layer temperature of the specimens being irradiated by IPEB achieves the melting point. The thickness of the remelted layer is on average about 100 microns and is close to the electron path. Moreover, the IPEB provides localization of the maximum value of the absorbed energy at a depth of approximately 1/3 of the electron path in the alloy [5,7,8]. Since the heating rate of the specimen is higher in the deeper surface layers it causes the explosion of some remelted material with further rapid cooling and the corresponding heat transfer to the host alloy. Such cooling is accompanied by ultrafast crystallization of the molten material, causing structural and phase transformation affecting the properties of the irradiated surface layer of the alloy. Fig. 1 shows the surface layer patterns of alloy 1380 and alloy 1933 after IPEB irradiation with the common morphological features for both alloys: you can see that the IPEB activity is accompanied by the emergence of

Table 1

Chemical composition (wt.%) of the 1933 and 1380 aluminum alloys

| | Mg | Cu | Zn | Si | Fe | Mn | Al |
|------|-----|-----|-----|-----|------|-----|------|
| 1933 | 1,9 | 1,0 | 6,9 | 0,1 | 0,15 | 0,1 | Bal. |
| 1380 | 0,6 | 3,9 | 0,1 | 0,9 | 0,5 | 0,7 | Bal. |

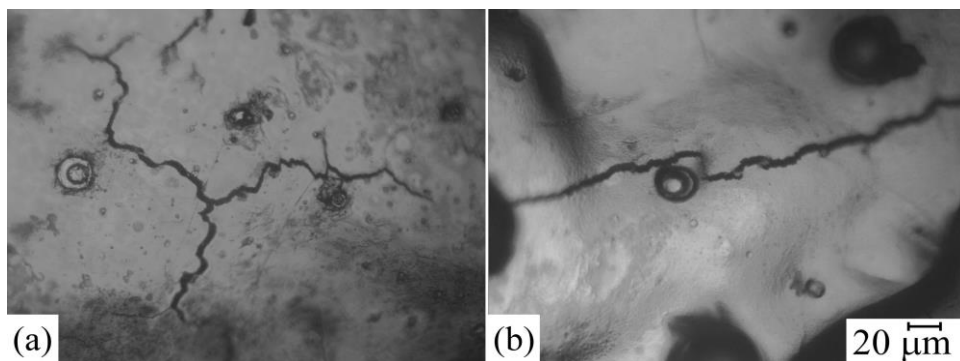


Fig. 1. Typical views of the irradiated surface layer of 1380 aluminum alloy (a) and 1933 aluminum alloy (b).

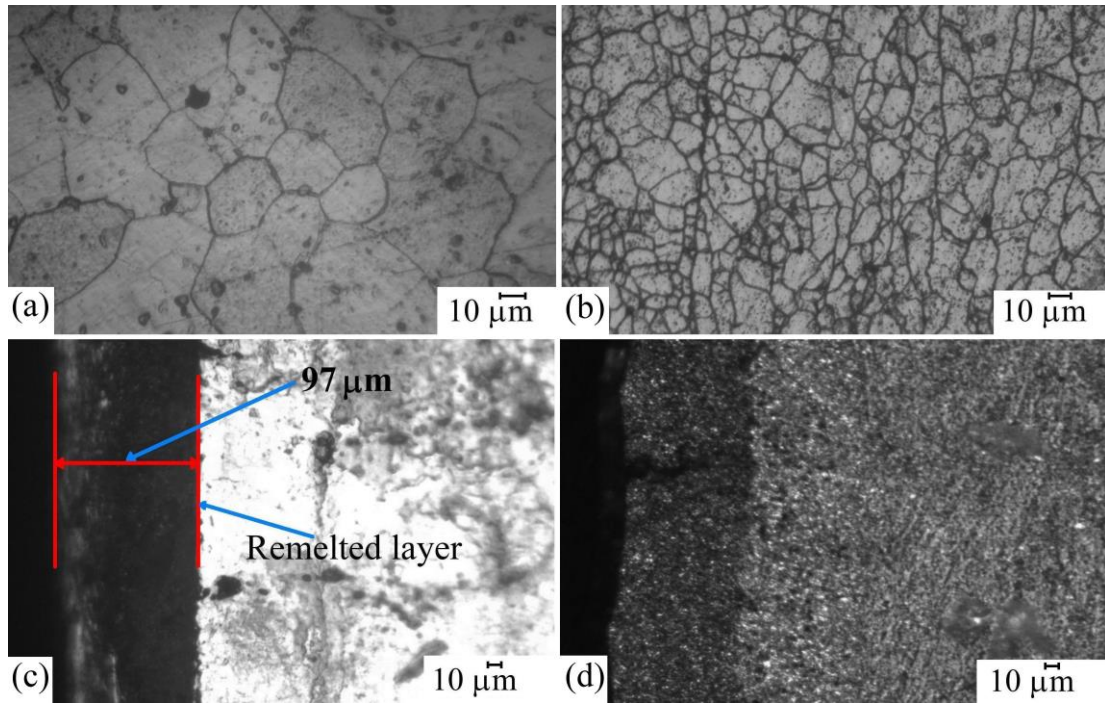


Fig. 2. Typical views of the initial grain microstructure of 1380 aluminum alloy (a) and 1933 aluminum alloy (b) and the cross-section morphology of 1380 aluminum alloy (c) and 1933 aluminum alloy (d) within the IPEB irradiated region.

the microcracks in the remelted surface layer. The reason for surface layer cracking is the thermoelastic stresses at the rapid crystallization. You can also observe emerged craters on some parts of the irradiated surface layer caused by the material emission at the gas release out of the surface layer.

It is claimed that the solidification of the melted surface layer at the wide range of temperature and high pressure caused a directed crystallization of the melt under non-equilibrium conditions and granted fine crystallite and amorphous structures [5-11]. Fig. 2 shows both views of the as-cast grain microstructure of the predetermined alloys and their cross-section of the region after IPEB irradiation. The average grain size of the irradiated alloy 1380 makes 31 microns with some inhomogeneity. The grains are mostly close to rounded (Fig. 2, a). The average grain size in alloy 1933 makes 15 microns (Fig. 2, b). As you can see in Fig. 2 (c, d) the thickness of the molten surface layer for both alloys makes approximately 100 microns. Thus the remelted surface depth does not depend on the as-cast grain size of the target alloys. The grain microstructure analysis confirms that the IPEB irradiation of alloy 1380 and alloy 1933 emerges the visible structure transformation of their surface layers.

Structural-phase transformations of the alloys after IPEB irradiation shall be the reason for their changing of the strength properties and first of all the micro-hardness ones. Fig. 3 shows alloy 1933 micro-hardness value distribution along the cross-section of the region affected by IPEB. The micro-hardness of the as-cast alloy makes 105HV0.05, a dashed line in Fig. 3. Fig.3 shows that the micro-hardness of the modified layer after IPEB irradiation increases dramatically and makes in average

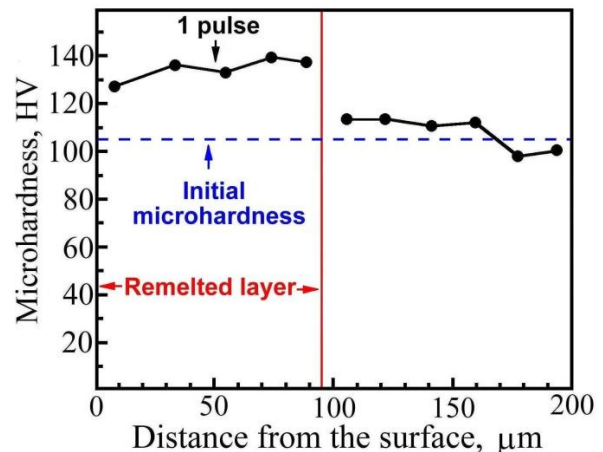


Fig. 3. 1933 aluminum alloy micro-hardness value distribution along the cross-section of the region affected by IPEB.

137HV0.05. Thus, we have proved that the IPEB irradiation causes the strengthening of the surface layer of alloy 1933 increasing the micro-hardness by 30% compared to the as-cast alloy. The micro-hardness values outside the remelted surface layer region of the IPEB affecting are dropping. However, these values remain higher than the ones of the as-cast alloy. Only the micro-hardness values at the approximate depth of 200 microns approach the values of the as-cast alloy.

Fig. 4 shows the micro-hardness distribution along the cross-section of the aluminum alloy 1380. The as-cast alloy 1380 micro-hardness makes 113HV0.05 (a dashed line in Fig. 4), but, as you can see in Fig.4, the micro-hardness of alloy 1380 after IPEB irradiation is

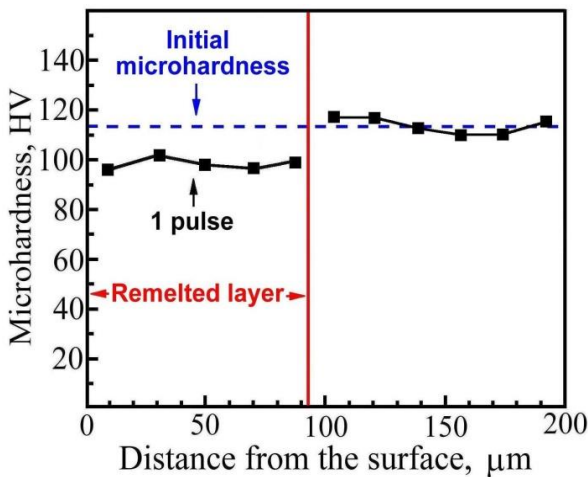


Fig. 4. 1380 aluminum alloy micro-hardness value distribution along the cross-section of the region affected by IPEB.

Decreasing and makes approximately 98HV0.05. Thus, we have proved that the IPEB irradiation causes the weakness of the surface layer of alloy 1380 decreasing the micro-hardness by 10% compared to the initial alloy. The alloy 1380 micro-hardness values outside the remelted surface layer region of the IPEB affecting are increasing. Within the region the micro-hardness values become a bit higher than the micro-hardness of the initial alloy. The micro-hardness values at the approximate depth of 200 microns from the surface layer approach the values of the initial alloy.

Thus, the experimental results show that the micro-hardness of the surface layer of alloy 1933 melted by IPEB increases, while for alloy 1380, the micro-hardness of the modified surface layer decreases. Differences in the micro-hardness value behavior of aluminum alloys 1933 and 1380 after IPEB treating along with the same energy parameters can be stipulated by the forthcoming emerged particularities of the structural and phase transformations.

III. Discussion on Strengthening Mechanisms

Hardness is the ability of a material to resist that deformation achieved from the indentation of a harder solid indenter onto a flat surface of metal under a load. The definition of hardness will allow us to make conclusions on the material strength and ductility [14]. To identify micro-hardness we study plastic deformation of aluminum and its alloys that occurred due to the dislocation motions. When dislocations meet a challenge on their way they cannot shear any more as earlier. The alloy strength properties responsible for the micro-hardness improvement and reduction are identified by the whole range of the strengthening mechanisms. Regularly the yield strength of aluminum alloys is described by the additive impacts of various strengthening mechanisms [15-18]:

$$\sigma_{0.2} = \sigma_0 + \sigma_1 + \sigma_2 + \sigma_3 + \sigma_4, \quad (1)$$

where σ_0 - is the yield strength of pure aluminum σ_1 - yield strength change due to the solid solution impact σ_2 - yield strength change due to the grain boundary strengthening; σ_3 - yield strength change due to dislocation hardening impact; σ_4 - yield strength change due to dispersion hardening impact.

To recognize properly the nature of the strengthening processes in the modified by IPEB surface layers we should perform contribution analysis to the strengthening mechanisms and consider the gained on the experimental basis qualitative and quantitative parameters of the grain microstructure of the melted surface layer of every predetermined alloy. At the same time, the main task is to establish the reasons causing alloy 1933 micro-hardness improving and alloy 1380 micro-hardness reduction after the equal IPEB affecting.

3.1. Solute Strengthening

Alloying element increase in a solid solution concentration can gain solute strengthening. This type of strengthening is fostered by the interaction between incoherent dislocations with distorted lattice atoms and the soluble ones causing such distortion [19]. The below equation evaluates a solute strengthening as follows [19]:

$$\sigma_1 = \sum_j k_j C_j^n, \quad (2)$$

where C_j is the concentration of the j dissolved element in the aluminum matrix, and n is a constant considering inhomogeneity of the dissolved element distribution within the alloy. The n constant can vary in the range from 0.5 to 0.75 [19], k_j is a ratio determined the dislocation integration with the j alloying element. To calculate k_j we shall apply the characteristics of the double aluminum alloy (e.g. Al-Cu, Al-Mg).

Referring to the equation we can see the higher concentration of the dissolved element the better is strengthening.

X-Ray Spectroscopy (EDS) distinguishes the inhomogeneous distribution of alloying elements within as-cast alloy 1933. Thus, we can observe Magnesium segregation at grain boundaries as a part of a number of intermetallic phases. Zinc and copper atoms are distributed in the aluminum-based solid solution more homogeneously than magnesium. The alloying element concentration in the modified surface layer is increasing after IPEB affecting of alloy 1933, but its alloying element distribution in solid solution is more homogeneous. The remelted by the IPEB treatment surface layer of the aluminum-based solid solution of alloy 1933 already contains Mg (0.4 wt.%), Cu (0.8 wt.%), and Zn (5.1 wt.%). Thus the aluminum-based solid solution is already a copper supersaturated one. The alloying element concentration in the modified surface layer is increasing after IPEB affecting of alloy 1380 as well, and the aluminum-based solid solution becomes a copper supersaturated one too. An increase in the concentration of alloying elements in the α -solid solution of alloys should lead to an increase in their strength.

Thus, the above-mentioned structure transformation for both alloy 1933 and alloy 1380 should have improved their micro-hardness [20]. But we should admit it is rather challenging to identify the strengthening mechanism impact of the multi-compound aluminum alloys due to the absence of a well-developed database of experimental data. The solid solution hardening mechanism is a core one for the aluminum alloys, whereas we cannot apply thermal strengthening [19]. However, the present paper contributes to the behavior research of the strengthening mechanisms applicable to the predetermined alloys and matters as well.

3.2. Grain Boundary strengthening

Grain boundaries are obstacles to the dislocation motions. When dislocations achieve the grain boundaries, they cannot slide in an insurmountable way any longer due to the different orientation of sliding systems between the adjacent crystallites. Consequently, the travel distance that incoherent dislocation can move before achieving the grain or crystallite boundary decreases with the grain size decreasing and thus, improving the hardening. This type of strengthening mechanism is called a grain-boundary strengthening. [21]. The Hall-Petch strengthening equation evaluates a grain-boundary strengthening impact as follows [21, 22]:

$$\sigma_2 = kd^{-0.5}, \quad (3)$$

where k is the index of the grain boundary hardening of Hall-Petch constant; d is average grain size.

The structure of the modified surface layer of the predetermined alloy extremely differs from the host alloy for its small submicron grain size. The as-cast grain size of alloy 1933 makes 15 microns, and the one of alloy 1380 makes 32 microns (Fig.2, a, b). After IPEB irradiation the grain size of the modified layer makes approximately 1 micron. Thus the travel distance the incoherent dislocation can move within the grain boundaries is significantly reduced. Therefore, such type of a strengthening mechanism makes a certain positive impact on the micro-hardness improvement of the predetermined alloys. Moreover, the micro-hardness increase for the alloy 1380 due to initial bigger grain size should be even slightly greater than for alloy 1933 based on the grain-boundary strengthening effect.

3.3. Dislocation Strengthening

The motion resistance of dislocations caused by stationary dislocations lying in the sliding planes and elastic interactions with dislocations lying in planes parallel to the sliding planes is estimated as follows [18]:

$$\sigma_3 = M\alpha Gb\sqrt{\rho}, \quad (4)$$

where α - is a dimensionless parameter approximately equal to 0.24 for aluminum alloys and considers the distribution behavior and the dislocation motion [18]; G is the shear modulus; b is the Burgers vector; M is the Taylor factor considering the number of sliding planes.

Rapid cooling of the remelted layer of the predetermined alloys after IPEB irradiation is

accompanied by the creating of elastic-plastic stress fields, which partial relaxation is accompanied by dislocation volume density and causes deformation bending e.g. emerging of a new substructure [5-13]. In compliance with the data of X-Ray structure analysis, the dislocation density of the surface layer after IPEB irradiation increases several times. Consequently, the strength increase of the surface layer of the predetermined alloys will also occur due to the dislocation volume density increase and new substructure formation.

3.4. Dispersion Hardening

This type of strengthening mechanism is caused by the interaction of incoherent dislocations with intermetallic phase particles present in alloys. Dispersion strengthening occurs due to the incoherent dislocation complication in their approach and attempts to climb through dispersoids. The way of interaction and the dispersion strengthening impact depends on the nature of the dispersoids. There are two ways of the creep behavior of both the incoherent dislocation and dispersoid interaction: to climb and to cut. The mechanism of dislocation & dispersoid interaction depends on their number, distribution, average size, and boundary coherence. Climbing way of the creep behavior is the second to none way for the dislocation and dispersoid interaction for the alloys subjected to the study of this paper. Hence, the dispersion hardening impact is expressed by Orowan's equation [15, 23]:

$$\sigma_{Orowan} = \frac{0,4MGb}{\pi L\sqrt{1-\nu}} \ln \frac{D}{b}, \quad (5)$$

where M is the Taylor factor; G is the shear modulus; b is the Burgers vector; L is the effective distance between particles; ν is the Poisson's coefficient; and D is the average particle diameter.

The effective distance between the particles is measured as follows [23]:

$$L = 0,4155 \left(\frac{F_v}{\pi r^3} \right)^{-1/3}, \quad (6)$$

where F_v is the amount of particles per unit volume, r is the average particle radius.

The predetermined alloys subjected to the study of the paper improve their strengthening via quenching and aging, whereas the highest strengthening level is provided by artificial aging. We applied X-ray Powder Diffraction (XRD) to determine the phase compound of both initial alloys and then their surface layer after IPEB irradiation.

Alloy 1380 may include dispersoids of Mg_2Si phase, Al_2CuMg phase, $CuAl_2$ phase as well as an insufficient amount of other phases [2]. Fig. 5 shows XRDs of initial alloy 1380 (1) and modified surface layer after IPEB irradiation, with intense diffraction peaks meeting the aluminum-based solid solution (α_{Al} -phase). The XDR of the as-cast alloy shows the peaks of $CuAl_2$, Mg_2Si and Al_2CuMg phases. Whilst the XDR of the surface layer

after IPEB irradiation contains only the peaks of phase α_{Al} , (true for alloy 1380). Particles of $CuAl_2$, Mg_2Si , and Al_2CuMg phases are dissolved at the recrystallization process during IPEB irradiation. Some small quantity of $CuAl_2$, Mg_2Si i Al_2CuMg phase particles, as well as a range of other phases, will be available in the modified surface layer after IPEB irradiation, however, the quantity is so insufficient, that we can omit them out of the research results.

Fig. 6 shows the XRD of initial alloy 1933 specimen (1) and the modified surface layer after IPEB irradiation, with intense diffraction peaks of as-cast alloy belong to (α_{Al} -phase), as well as the peaks of $MgZn_2$, $Al_2Mg_3Zn_3$ and Al_2CuMg phases.

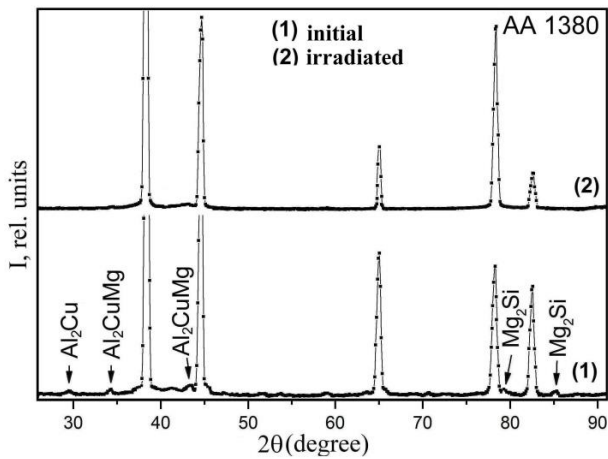


Fig. 5. XRD of the initial alloy 1380 specimen (1) and the remelted surface layer after IPEB irradiation (2).

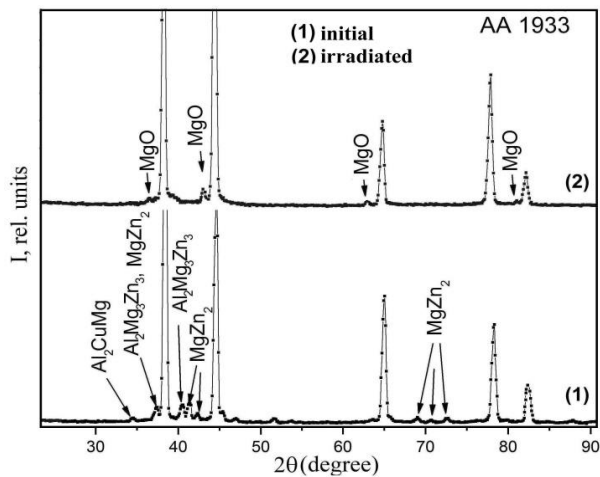


Fig. 6. XRD of the initial alloy 1933 specimen (1) and its remelted surface layer after IPEB irradiation (2).

Some peaks are failed to be identified in the XDR but we can predict that the peaks at 51.5° and 53.4° will belong to Al_3Zr phase [24]. The phase particle can be available in alloy 1933 [1]. Whilst the XDR of the remelted surface layer after IPEB irradiation contains the intense diffraction peaks meeting α_{Al} phase, (true for alloy 1933). The XRD does not contain any peaks meeting $MgZn_2$, $Mg_3Zn_3Al_2$, and Al_2CuMg phases, available in the as-cast alloy. That means if these phases

are available in the remelted surface layer after IPEB irradiation they will be available in extremely insufficient amounts. However, the XDR shows some magnesium oxide peaks, the evidence of the MgO presence in the modified surface layer after IPEB irradiation.

The particularities of the magnesium oxide impurity distribution within the grain microstructure of the remelted surface layer after IPEB irradiation were investigated via a Scanning Electron Microscope (SEM) and investigated due to the Energy Dispersive X-Ray Spectroscopy (EDS). Fig. 7 shows a view of the polished surface of the remelted surface of alloy 1933. We selected the impurities of the light shade typical for magnesium oxide to determine the chemical composition. You can see a digit 1 stipulated for MgO impurities. We found that the MgO of light shade came with a high concentration of both oxygen and magnesium exceeding the average alloy concentration more than 10 times (Fig. 7, b) The typical ratio for the oxygen and magnesium weight allows us to suggest that there is the localization of the magnesium oxide. Metallographic analysis has shown that the size of MgO impurities makes from 50 to 500 nm at an average distance from 1 to 5 microns. You can see their homogeneous distribution within the polished cut of the specimen.

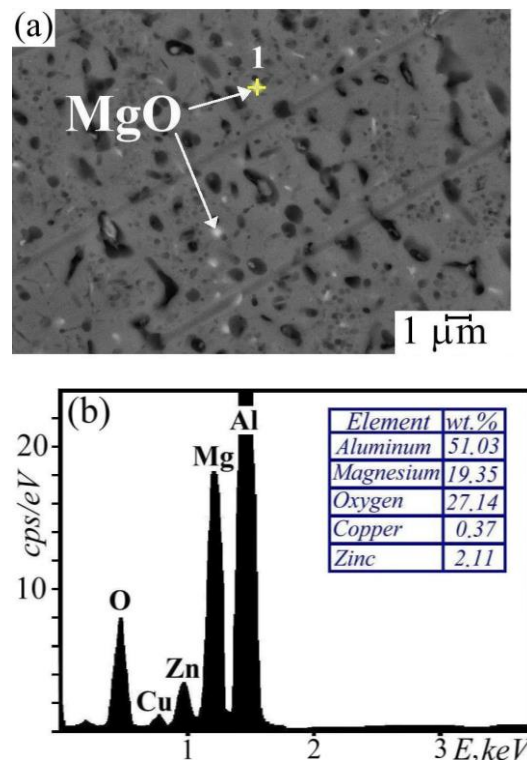


Fig. 7. The view of the grain microstructure of the remelted surface layer of alloy 1933 at the depth of 30 microns from the top of the surface - (a); EDS image of Al, Zn, Mg, Cu, and O from Point 1 (Fig. 7, a - b).

Thus both initial alloy 1933 and alloy 1380 are multiphase ones. The IPEB irradiation of the alloy surface layer is accompanied by the drastic grain microstructure altering of the surface layer itself. Therefore we can observe the formation of the alloy surface layer with a submicrocrystalline structure with its core phase is an aluminum-based solid solution. Almost

all intermetallic phases being present in the as-cast alloys are dissolved due to the IPEB irradiation. However, in the remelting of the surface layer of alloy 1933, we will observe the emerging of magnesium oxide crystalline impurities, we suggest they, themselves, are the keystone of the micro-hardness improvement of the remelted layer of this alloy. At the same time, the surface layer of alloy 1380 after IPEB irradiation due to the complete dissolution of the secondary phase particles is weakened.

To understand the mechanisms of the MgO impurity formation in the remelted surface layer we should study the dynamics and conditions of the IPEB process. The IPEB activity causes the surface micro blast to occur which is accompanied by a shock-plastic wave expanding towards the target and the material emission towards the beam activities. Irradiation is carried out inside the accelerator vacuum chamber at a pressure of $10^{-4} \dots 10^{-5}$ Tor. At this pressure, the oxidation processes of alloys will occur due to the presence of oxygen in the residual vacuum medium. The gases out of the residual vacuum medium of the operational chamber participate in the mixing of the surface layer whilst it is being in the molten state. As a result, the surface layer is the media to be form oxides with the oxygen attractive elements of the target.

Due to the same conditions and the same range of IPEB energy affecting the forming of the magnesium oxides occurring only in alloy 1933 is possibly subjected to the availability of the magnesium amount in the alloy ligature. It is known that the initial product at the beginning of the oxidation of the molten aluminum alloy containing more than 1 wt. % magnesium is MgO [25, 26]. The magnesium amount in alloy 1933 exceeds the weight by two times. Whereas alloy 1380 contains a significantly lower amount (0.6 wt.%) of magnesium, which is concentrated in the aluminum-based solid solution in the only phase of Mg_2Si that is subjected to be dissolved completely. Consequently, the magnesium oxides are not identified through XRD research methods studying the remelted surface of alloy 1380. Magnesium is concentrated basically in intermetallic impurities of $MgZn_2$, $Mg_3Zn_3Al_2$ and Al_2CuMg and in segregations to be crushed and instantly oxidized at the irradiation moment. Dispersed MgO particles formed at the irradiation get into the surface layer, which quickly crystallizes.

We found out the general MgO particle impact on the strengthening of aluminum alloy 1933. We calculate the particle size and effective distance between the particles based on metallographic analysis data. The Orowan ratio describes the magnesium oxide particle servicing as obstacles for the dislocation motion within the aluminum matrix as well as their impact on the strengthening. We found that the strengthening caused by the MgO availability in the alloy 1933 structure is approximately 87 MPa.

Thus, all the above strengthening mechanisms e.g. solid solution hardening, grain-boundary strengthening, and dislocation strengthening contribute to the strengthening improvement in a positive way for the irradiated surface layer. However, it is the dispersion hardening that plays a key role in the strength changing

of the modified surface layers of the predetermined alloys. Due to the dissolution of secondary phase particles during irradiation, the surface of alloy 1380 is weakened, which leads to a decrease in its micro-hardness. Weakening due to the dissolution of the secondary phases in the surface layer of alloy 1933 is compensated by the strengthening due to the magnesium oxide particle forming caused by the irradiation. Summarizing the total micro-hardness of the surface layer of alloy 1933, we found it increases due to the structure and phase transformations at the IPEB irradiation.

Conclusion

The IPEB irradiation of the predetermined alloys causes the forming of the surface layer with the submicrocrystalline structure with the core phase of the aluminum-based solid solution. Intermetallic phases being present in the as-cast alloys are not detected by XRD methods in the surface layer after IPEB irradiation. However, the crystalline MgO impurities being absent in the as-cast alloy are formed in the remelted surface layer of alloy 1933 after IPEB irradiation. But there are no MgO particles in the remelted surface layer of alloy 1380.

The micro-hardness of the remelted surface layer of alloy 1933 comes up at the same terms and conditions whilst the micro-hardness of alloy 1380 comes down. Differences in the micro-hardness value behavior of aluminum alloy 1933 and alloy 1380 after IPEB irradiation along with the same energy parameters can be stipulated by the available differences of the occurring structure and phase transformations. Although the studied alloys come with the same alloying elements, the keystone of altering the physical and technological properties is the magnesium amount in the alloy ligature.

Based on the experimentally identified quantitative and qualitative parameters of the structure, we recognized the physical nature of the strengthening alteration of the remelted surface layers after IPEB irradiation of alloy 1933 and alloy 1380. We show a variety of strengthening mechanisms participating in the process and altering the alloy operational properties. The main role in the alloy strengthening transformation plays the Orowan dispersion hardening impact describing the way the crystalline magnesium oxide impurities contributing to the improved micro-hardness of the remelted surface layer of alloy 1933.

Bryukhovetsky V.V. -Dr. Sci., Senior Research, head of department;

Lytvynenko V.V. -Dr. Sci., Senior Research, Managing Director;

Myla D.E. -Ph. D., Research;

Bychko V.A. -Ph. D., Docent, Associate Professor of Department of Information and Computer Systems;

Lonin Yu.F. -Dr.Sci., Senior Research, Head of Department NSC KIPT NAS of Ukraine

Ponomarev A.G. -Ph.D., head of laboratory;

Uvarov V.T. -Ph.D., Senior Research, Senior Research.

- [1] I.N. Fridlyander, A.V. Dobromyslov, E.A. Tkachenko, O.G. Senatorova, *Metal Science and Heat Treatment* 47(7-8), 269 (2005); <https://doi.org/10.1007/s11041-005-0066-7>.
- [2] N.A. Belov, N.N. Avksent'eva, *Metal Science and Heat Treatment* 55(7-8), 358 (2013); <https://doi.org/10.1007/s11041-013-9635-3>.
- [3] V.P. Poida, D.E. Pedun, V.V. Bryukhovetskii, A.V. Poida, R.V. Sukhov, A.L. Samsonik, V.V. Litvinenko, *The Physics of Metals and Metallography* 114(9), 779 (2013); <https://doi.org/10.1134/S0031918X13070090>.
- [4] V.V. Bryukhovetsky, A.V. Poyda, V.P. Poyda, D.E. Milaya, *Problems of Atomic Science and Technology* 114, 94 (2018).
- [5] V.V. Bryukhovetsky, V.F. Klepikov, V.V. Lytvynenko, D.E. Myla, V.P. Poyda, A.V. Poyda, V.T. Uvarov, Yu.F. Lonin, A.G. Ponomarev, *Nuclear Inst. and Methods in Physics Research B* 499, 25 (2021); <https://doi.org/10.1016/j.nimb.2021.02.011>.
- [6] V.V. Bryukhovetskiy, N.I. Bazaleev, V.F. Klepikov, V.V. Litvinenko, O.E. Bryukhovetskay, E.M. Prokhorenko, V.T. Uvarov, A.G. Ponomar'ov, *Problems of Atomic Science and Technology* 72, 28 (2011).
- [7] Y. Qin, C. Dong, Z. Song, S. Hao, X. Me, J. Li, X. Wang, J. Zou, Th. Grosdidier, *J. Vac. Sci. Technol. A* 27(3), 430 (2009); <http://dx.doi.org/10.1116/1.3093876>.
- [8] B. Gao, S. Hao, J. Zou, W. Wu, G. Tu, C. Dong, *Surface & Coatings Technology* 201, 6297 (2007); <http://dx.doi.org/10.1016/j.surfcoat.2006.11.036>.
- [9] V.T. Uvarov, V.V. Uvarov, V.N. Robuk, N.I. Bazaleev, A.G. Ponomarev, A.N. Nikitin, Yu.F. Lonin, T.I. Ivankina, V.F. Klepikov, V.V. Lytvynenko, S.Ye. Donets, *Phys. of Part. and Nucl. Latter.* 11(3), 274 (2014); <http://dx.doi.org/10.1134/S1547477114030157>.
- [10] Y. Hao, B. Gao, G.F. Tu, S.W. Li, C. Dong, Z.G. Zhang, *Nuclear Inst. and Methods in Physics Research, B* 269, 1499 (2011); <https://doi.org/10.1016/j.nimb.2011.04.010>.
- [11] D.E. Myla, V.V. Bryukhovetsky, V.V. Lytvynenko, V.P. Poyda, A.V. Poyda, V.F. Klepikov, V.T. Uvarov, Yu.F. Lonin, A.G. Ponomarev, *Problems of Atomic Science and Technology* 126, 33 (2020).
- [12] V.V. Bryukhovetsky, A.V. Poyda, V.P. Poyda, D.E. Milaya, *Problems of Atomic Science and Technology* 120, 67 (2019).
- [13] D.I. Proscurovsky, A.D. Pogrebnjak, *Phys. Stat. Sol. A* 145(1), 9 (1994); <https://doi.org/10.1002/pssa.2211450103>.
- [14] D. Tabor, *Phil. Mag. A* 74(5), 1207 (1996); <http://doi.org/10.1080/01418619608239720>.
- [15] L.M. Brown, R.K. Ham. In *Strengthening Methods in Crystals*, Ed. A. Kelly, R.B. Nicholson (Elsevier: Amsterdam, The Netherlands, 1971).
- [16] L.F. Mondolfo, J.G. Barlcok. *Metallurgical Transactions B (Process Metallurgy)* 6, 565 (1975); <https://doi.org/10.1007/BF02913849>.
- [17] E.L. Huskins, B. Cao, K.T. Ramesh, *Mater. Sci. Eng. A* 527, 1292 (2010); <https://doi.org/10.1016/j.msea.2009.11.056>.
- [18] N. Kamikawa, X. Huang, N. Tsuji, N. Hansen, *Acta Materialia* 57, 4198 (2009); <http://doi.org/10.1016/j.actamat.2009.05.017>.
- [19] O. Ryen, O. Nijs, E. Sjolander, B. Holmedal, H.-E. Ekstrom, E. Nes, *Metall. Mater. Trans. A* 37, 1999 (2006); <https://doi.org/10.1007/s11661-006-0142-7>.
- [20] L.M. Pike, Y.A. Chang, C.T. Liu, *Acta Materialia* 45(9), 3709 (1997); [https://doi.org/10.1016/S1359-6454\(97\)00028-1](https://doi.org/10.1016/S1359-6454(97)00028-1).
- [21] N. Hansen, *Scripta Mater* 51, 801 (2004); <https://doi.org/10.1016/j.scriptamat.2004.06.002>.
- [22] M. Kato, *Materials Transactions* 55, 19 (2014); <https://doi.org/10.2320/matertrans.MA201310>.
- [23] K.L. Kendig, D.B. Miracle, *Acta Materialia* 50, 4165 (2002); [https://doi.org/10.1016/S1359-6454\(02\)00258-6](https://doi.org/10.1016/S1359-6454(02)00258-6).
- [24] K.E. Nipling, D.C. Dunand, D.N. Seidman, *ZeitschriftfürMetallkunde* 97(3), 246 (2006); <https://doi.org/10.3139/146.101249>.
- [25] A.V. Poyda, V.V. Bryukhovets'ky, D.L. Voronov, R.I. Kuznetsova, V.F. Klepikov, *Metallofiz. Noveishie Tekhnol.* 27(3), 317 (2005).
- [26] K. Kim, *Surface and Interface Analysis* 47(4), 429 (2015); <https://doi.org/10.1002/sia.5726>.

В.В. Брюховецький¹, В.В. Литвиненко¹, Д.Є. Мила¹,
В.А. Бичко², Ю.Ф. Лонін³, А.Г. Пономарьов³, В.Т. Уваров³

Вплив структурно-фазових змін при опроміненні імпульсним пучком релятивістських електронів на мікротвердість алюмінієвих сплавів

¹Інститут електрофізики і радіаційних технологій НАН України, Харків, Україна, bvv260170@ukr.net

²Національний університет «Чернігівська політехніка», Чернігів, Україна

³Національний науковий центр «Харківський фізико-технічний інститут» НАН України, Харків, Україна

Вивчено особливості зміни значень мікротвердості промислових алюмінієвих сплавів 1933 і 1380 в зоні обробки імпульсним пучком електронів. Поверхневий шар сплавів був модифікований дією пучка електронів з однаковими енергетичними параметрами. Проте фізико-технологічні властивості опроміненого шару сплавів мали деякі відмінності. Показано, що для сплаву 1933 мікротвердість модифікованого шару збільшується більш ніж на 30 %, а для сплаву 1380 мікротвердість переплавленого шару зменшується на 10 %. Проаналізовано механізми, які впливають на зміну міцності металевих матеріалів, оброблених імпульсним електронним пучком. Встановлено, що одним з основних фактором підвищення мікротвердості поверхневого шару сплаву 1933 є утворення в ході опромінення дрібнодисперсних частинок MgO, які були відсутні в початковому стані сплаву. У той же час мікротвердість опроміненого шару сплаву 1380 зменшується через розчинення в процесі опромінення зміцнюючих фаз, які були ідентифіковані у початковому стані.

Ключові слова: мікротвердість, опромінення, структурно-фазові зміни, алюмінієві сплави.